Volume 9 | Issue 3 Article 20

Eggshell-alginate composites (EACs) as eco-friendly adsorbents for Rhodamine B uptake from aqueous solutions

Rusnadi Rusnadi
Analytical Chemistry Research Group, Bandung Institute of Technology, Jl. Ganesha 10, Bandung 40132, Indonesia, rusnadi@itb.ac.id

Mar'atus Sholihah
Analytical Chemistry Research Group, Bandung Institute of Technology, Jl. Ganesha 10, Bandung 40132, Indonesia.

Nurrahmi Handayani
Research Unit for Environment and Clean Technology, National Research and Innovation Agency, Jl. Cisitu, Sangkuriang, Ban-dung 40135, Indonesia

Muhammad Ali Zulfikar
Analytical Chemistry Research Group, Bandung Institute of Technology, Jl. Ganesha 10, Bandung 40132, Indonesia.

Eggshell-alginate composites (EACs) as eco-friendly adsorbents for Rhodamine B uptake from aqueous solutions

Abstract

The contamination of wastewater by Rhodamine B (RhB) poses a significant environmental concern due to its negative impacts on aesthetics, ecosystems, and human well-being. This study successfully synthesized eco-friendly egg-shell-alginate composites (EACs) as adsorbents by combining alginate solution, eggshell powder, and a 2% CaCl2 solu-tion. Characterization techniques including FTIR, SEM, TGA, and SAA were employed to analyze the EACs. FTIR analysis revealed characteristic absorption peaks corresponding to -OH groups, C=O groups, C-O groups, and the pres-ence of CO32-. The structural analysis confirmed the physical mixture of functional groups from eggshells and alginate, resulting in a homogeneous EACs mixture. TGA analysis demonstrated the decomposition of eggshell calcium car-bonate (CaCO3), yielding calcium oxide (CaO) and carbon dioxide (CO2) within the 700-800°C temperature range. SAA results indicated that EACs exhibited a mesoporous structure (average pore diameter: 20-500 Å) and a higher sur-face area (6.102 m2/g) compared to eggshells. The adsorption capacity of EACs for RhB was investigated by evaluating contact time, adsorbent dosage, pH, and initial concentration. Characterization results validated the successful synthesis of EACs with enhanced thermal resistance compared to Ca-alginate. Sorption studies demonstrated the potential of EACs as effective adsorbents for RhB removal from aqueous solutions, following the Langmuir isotherm model with a maximum adsorption capacity of 151.51 mg/g. Furthermore, adsorption kinetics exhibited a pseudo-second-order mod-el. Thermodynamic analysis indicated that RhB adsorption onto EACs was exothermic (negative ΔHo) and spontaneous (negative ΔGo). The results underscore the potency of EACs as highly efficient adsorbents for the remediation of RhB-contaminated water bodies.

Keywords

eggshell/alginate, Rhodamine B removal, adsorption, eco-friendly adsorbents

RESEARCH PAPER

Eggshell-alginate Composites (EACs) as Eco-friendly Adsorbents for Rhodamine B Uptake from Aqueous Solutions

Rusnadi Rusnadi [a,*], Mar'atus Sholihah [a], Nurrahmi Handayani [a,b], Muhammad A. Zulfikar [a]

[a] Analytical Chemistry Research Group, Bandung Institute of Technology, Jl. Ganesha 10, Bandung 40132, Indonesia
[b] Research Unit for Environment and Clean Technology, National Research and Innovation Agency, Jl. Cisitu, Sangkuriang, Bandung 40135, Indonesia

Abstract

The contamination of wastewater by Rhodamine B (RhB) poses a significant environmental concern due to its negative impacts on aesthetics, ecosystems, and human well-being. This study successfully synthesized eco-friendly eggshell-alginate composites (EACs) as adsorbents by combining alginate solution, eggshell powder, and a 2% $CaCl_2$ solution. Characterization techniques including FTIR, SEM, TGA, and SAA were employed to analyze the EACs. FTIR analysis revealed characteristic absorption peaks corresponding to −OH groups, C=O groups, C−O groups, and the presence of CO_3^{2-}. The structural analysis confirmed the physical mixture of functional groups from eggshells and alginate, resulting in a homogeneous EACs mixture. TGA analysis demonstrated the decomposition of eggshell calcium carbonate ($CaCO_3$), yielding calcium oxide (CaO) and carbon dioxide (CO_2) within the 700−800 °C temperature range. SAA results indicated that EACs exhibited a mesoporous structure (average pore diameter: 20−500 Å) and a higher surface area (6.102 m^2/g) compared to eggshells. The adsorption capacity of EACs for RhB was investigated by evaluating contact time, adsorbent dosage, pH, and initial concentration. Characterization results validated the successful synthesis of EACs with enhanced thermal resistance compared to Ca-alginate. Sorption studies demonstrated the potential of EACs as effective adsorbents for RhB removal from aqueous solutions, following the Langmuir isotherm model with a maximum adsorption capacity of 151.51 mg/g. Furthermore, adsorption kinetics exhibited a pseudo-second-order model. Thermodynamic analysis indicated that RhB adsorption onto EACs was exothermic (negative ΔH^o) and spontaneous (negative ΔG^o). The results underscore the potency of EACs as highly efficient adsorbents for the remediation of RhB-contaminated water bodies.

Keywords: Eggshell/alginate, Rhodamine B removal, Adsorption, Eco-friendly adsorbents

1. Introduction

Rhodamine B (RhB) is a ubiquitous synthetic dye used in various industries, including paint, leather, paper, and textiles [1,2]. However, its remarkable stability, resistance to degradation, and toxic nature pose significant challenges when it enters the environment, leading to aesthetic, environmental, and health concerns [3]. As a result, addressing the presence of RhB in wastewater becomes a pressing issue, necessitating effective and efficient treatment to mitigate its potential hazards.

Numerous technologies have been explored for RhB dye removal, including coagulation [4], biological processes [5], membrane treatments [6], and photocatalytic degradation [7]. Among these methods, adsorption has emerged as one of the most extensively studied approaches due to its simplicity and effectiveness [4]. Nevertheless, the quest for an environmentally friendly adsorbent with exceptional adsorption capacity and stability remains a persistent challenge.

Several recent articles have emphasized the importance of developing effective adsorbents for the

Received 16 March 2023; revised 14 July 2023; accepted 16 July 2023.
Available online 21 September 2023

* Corresponding author.
E-mail address: rusnadi@itb.ac.id (R.Rusnadi).

https://doi.org/10.33640/2405-609X.3317

removal of Rhodamine B (RhB) from aqueous solutions. Notably, Chen et al. [8] investigated the adsorption capacity of activated carbon nanotubes, highlighting the need for advanced materials with high adsorption efficiency. Similarly, Tuzen et al. [9] explored the use of magnetic AC/CeO_2 nanocomposites as adsorbents for RhB, demonstrating the potential of nanomaterials in wastewater treatment. Alswieleh [10] focused on mesoporous silica nanoparticles and their adsorption performance for RhB, underscoring the significance of tailored adsorbents. Additionally, various materials such as zeolites, silica beads, activated carbon, bentonite, starch, coconut shell, and rice husk have been reported as potential adsorbents for RhB removal [11,12]. These studies collectively highlight the urgent need for innovative adsorbents capable of effectively removing RhB from aqueous solutions. Building on these research findings, the present study aims to investigate the adsorption potential of eggshell-alginate composites (EACs) as an eco-friendly and cost-effective adsorbent for RhB uptake.

In line with green principles, the utilization of eggshells as an adsorbent has gained attention due to their cost-effectiveness, eco-friendliness, and biodegradability [13]. Prior studies have highlighted the adsorption capacity of eggshell powder for heavy metal ions and organic pollutants [13,14]. However, the inherent limitations of eggshells, such as solubility at low pH, hinder their application as adsorbents under acidic conditions [15]. To overcome this hurdle, the modification of eggshells with calcium alginate emerges as a viable solution to create eggshell-alginate composites (EACs) that enhance stability and performance.

Alginate, a natural polysaccharide derived from dried brown algae, is renowned for its remarkable properties, including non-toxicity, affordability, and gel formation when exposed to divalent cations like Ca^{+2} [16,17]. By encapsulating eggshells within alginate, the resulting EACs offer enhanced stability and serve as efficient adsorbents.

This study presents a novel approach by modifying eggshells with calcium alginate, producing stable eggshell-alginate composites (EACs) as exceptional adsorbents. In contrast to conventional eggshells, the EACs overcome limitations such as solubility at low pH. The primary objective of this research is to investigate the remarkable adsorption potential of EACs for Rhodamine B (RhB) dyes, considering crucial factors such as contact time, EACs dosage, initial dye concentration, pH, and temperature. Moreover, the study explores the adsorption isotherm, thermodynamic, and kinetic properties associated with the adsorption process. This research contributes to the utilization of modified eggshells for enhanced adsorption capabilities, offering valuable insights into their application in wastewater treatment and environmental remediation. The effects of contact time, EACs dosage, initial dye concentration, pH, and temperature were evaluated in aqueous solutions.

2. Materials and methods

2.1. Materials

In the present study, all reagents used were of analytical grade. Rhodamine B (RhB), hydrochloric acid (HCl), anhydrate calcium dichloride (anh. $CaCl_2$), sodium hydroxide (NaOH), and sodium alginate were purchased from Merck (Germany).

2.2. Preparation of eggshell-alginate composites (EACs)

Discarded eggshells were collected from household waste. After being cleaned and washed, the eggshells were placed in an oven at 100 °C for 5 h. The dried eggshells were ground and washed with demineralized water. Subsequently, the dry eggshell powder was further dried in the oven at 100 °C for 8 h and sifted to obtain particles with a mesh size of 80. To prepare the eggshell-alginate composites, 4 g of eggshell powder were dispersed into a solution containing 2 g of sodium alginate in 100 mL of demineralized water. The mixture was stirred for 2 h until a homogeneous mixture was formed. This mixture was then slowly dripped into a 2% $CaCl_2$ solution to form composite granules. The resulting precipitates were separated and washed multiple times with demineralized water. The composite granules were subsequently dried at room temperature for 48 h and further dried in an oven at 60 °C for 5 h.

2.3. Characterization methods

The functional groups present in the synthesized EACs were characterized using a Shimadzu IR Prestige-21 Fourier Transform Infrared (FTIR) spectrometer. Thermal analysis was performed using a LINSEIS TGA PT-1000 thermogravimetric analyzer (TGA) with a temperature rise rate of 20 °C/min and a maximum temperature of 900 °C. The surface and matrix morphologies were observed using a JEOL JSM-6510 LA scanning electron microscope (SEM) at magnifications of 5000 times. Surface area and pore analysis were conducted using a NOVA 3200e Quantachrome surface

area analyzer (SAA), followed by analysis using the Brunauer-Emmet-Teller (BET) and Barret-Joyner-Halenda (BJH) methods.

2.4. Sorption studies

The adsorption study involved the batch technique to determine the adsorption capacity, thermodynamics, kinetic model, and isotherm model of Rhodamine B (RhB) adsorption by EACs. Adsorption measurements were conducted by mixing different amounts of EACs as adsorbents in Erlenmeyer flasks containing 25 mL of RhB solution at varying pH levels. The mixtures were stirred using a magnetic stirrer at 100 rpm for 3 h on a hot plate. The effect of several parameters such as the composition ratio of eggshells and alginates (1:1, 1:2, 1:4, 2:1, and 4:1), contact time (15–240 min), pH (2–7), adsorbent dose (0.05–1 g), initial dye concentration (5–500 ppm), and temperature (26–60 °C) was investigated.

The filtrate obtained after filtration was analyzed using a UV–Vis Spectrophotometer. The adsorption capacity (qe) was calculated using the equation:

$$q_e = \frac{C_o - C_e}{w} V \quad (1)$$

where q_e is the adsorption capacity (mg/g), C_o is the concentration of RhB (mg/L), C_e is the final concentration of RhB (mg/L), V is the volume of RhB solution (L), and w is the mass of adsorbent (g). The results were also evaluated by thermodynamic studies, simulation of adsorption kinetics models, and various adsorption isotherms including Langmuir, Freundlich, and Sips isotherms.

3. Results and discussions

3.1. Characteristics of the eggshell-alginate composites (EACs)

3.1.1. FTIR spectra

The infrared characterization of EACs, eggshells, and Ca-alginate in the range of 450–5000 cm^{-1} is presented in Fig. 1. In the spectra of Ca-alginate, a broad absorption peak at 3426 cm^{-1} corresponds to the characteristic vibration of the –OH group. Additionally, an absorption band at 1027 cm^{-1} indicates the presence of a C–O group, and an absorption region around 1613 cm^{-1} is attributed to the presence of a C]O group. The FTIR spectrum of the eggshell exhibits a strong absorption peak at 1425 cm^{-1}, which indicates the presence of a C]O group originating from CO_3^{2-} in the eggshell.

The FTIR spectrum of EACs displays a broad absorption peak at 3444 cm^{-1}, which is attributed to the –OH group. Furthermore, absorption peaks at 1608 cm^{-1}, 1027 cm^{-1}, and 1427 cm^{-1} indicate the presence of C]O, C–O, and CO_3^{2-} groups, respectively. The structural analysis confirms that the functional groups in EACs result from the combination of functional groups present in eggshells and alginate. This suggests that there is no chemical reaction, only physical mixing, resulting in a homogeneous mixture.

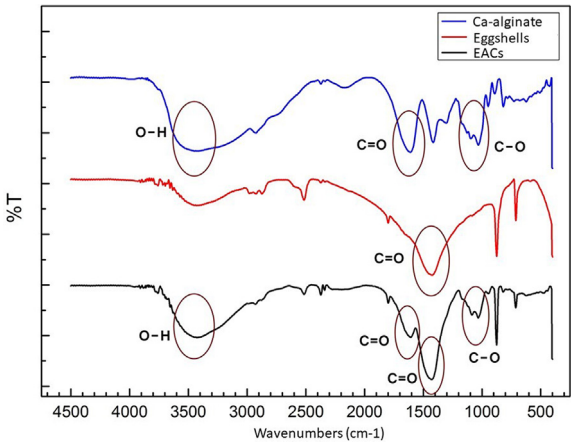

Fig. 1. FTIR spectrum of Ca-alginate, eggshells, and synthesized EACs.

Please refer to Fig. 1 for a visual representation of the infrared characterization of EACs, eggshells, and Ca-alginate in the specified wave number range of 450–5000 cm^{-1}.

3.1.2. TGA

Thermal resistance analysis using a Thermogravimetric Analyzer (TGA) was conducted to examine the behavior of eggshell powder, Ca-alginate, and EACs as the temperature increased. The TGA characterization was carried out up to a maximum temperature of 900 °C, as depicted in Fig. 2. The three samples exhibited distinct thermal behaviors in different temperature ranges.

For the eggshells, there was no significant mass reduction observed in the temperature range of 200–400 °C. However, both EACs and Ca-alginate displayed a notable decrease in mass within this temperature range. Furthermore, at temperatures between 700 and 800 °C, both eggshells and EACs exhibited a substantial mass reduction, indicating the decomposition of the primary component, $CaCO_3$, found in the eggshells, leading to the formation of CaO and CO_2. These findings highlight the thermal decomposition process occurring in the eggshell and the resultant changes in mass.

The results of the TGA analysis also demonstrate that EACs possess thermal properties that combine characteristics from both Ca-alginate and eggshells.

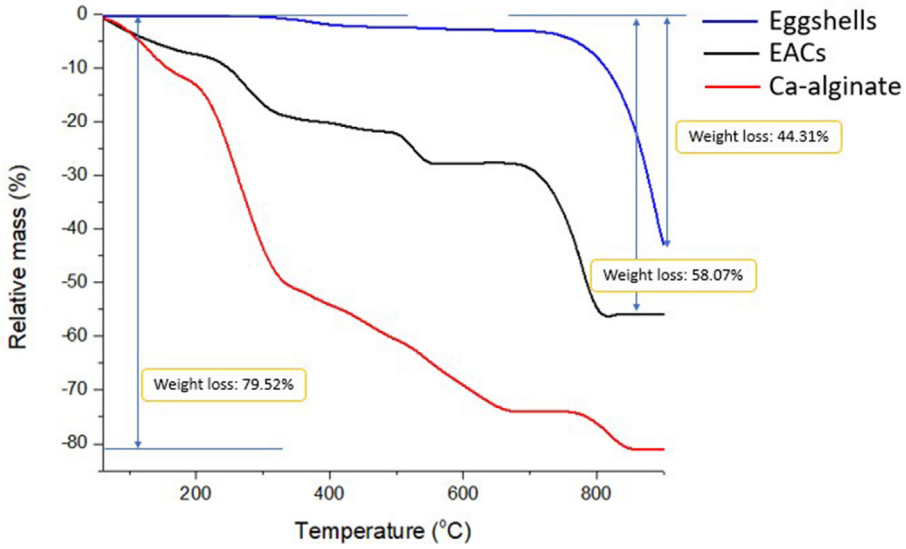

Fig. 2. Thermogram of eggshells, Ca-alginate, and EACs.

This indicates the successful formation of the EACs, where the thermal behavior reflects a synergistic combination of the individual components, enhancing the overall thermal resistance.

3.1.3. SEM

Fig. 3 illustrates the scanning electron microscopy (SEM) images of eggshell powder, Ca-alginate, and EACs, providing insights into their surface morphologies. The SEM analysis allows for a detailed examination of the structural characteristics of the materials.

In Fig. 3a, the SEM image of the raw eggshell powder reveals an irregular surface morphology with noticeable variations in pore sizes and coarse grain structures. These observations indicate the presence of inherent irregularities and roughness in the raw eggshell material. Comparatively, Fig. 3b displays the SEM image of Ca-alginate, which exhibits a smoother and more uniform surface morphology in comparison to the raw eggshell powder. The Ca-alginate structure shows relatively smaller and more evenly distributed pores, suggesting a more refined and controlled composition.

Notably, Fig. 3c showcases the SEM image of EACs, where a distinct particle structure with thick and porous edges can be observed. This morphology suggests that the synthesis process of combining eggshell powder and Ca-alginate has resulted in the development of well-defined composite particles. The presence of such porous edges in EACs indicates their potential as effective adsorbents, as increased surface area and porosity are desirable for efficient adsorption processes.

3.1.4. Surface area analyzer

Surface area analysis of the adsorbent was conducted using the BET (Brunauer-Emmet-Teller) method, and the pore properties were analyzed using the BJH (Barrett–Joyner–Halenda) method. Nitrogen adsorption/desorption isotherms were employed to determine the BET surface area and BJH pore volume. The results of this analysis are presented in Table 1.

Upon examination of Tables 1, it is evident that the synthesized EACs exhibit mesoporous characteristics, with an average pore diameter ranging from 20 to 500 Å. These mesopores contribute to the

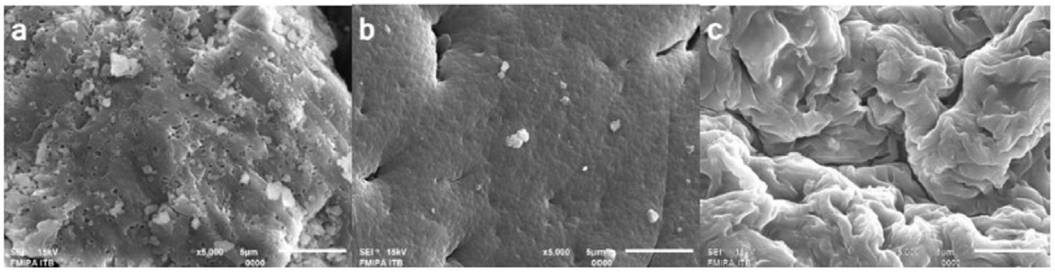

Fig. 3. SEM image of a) eggshell powder b) Ca-Alginate and c) EACs with the magnification of 5000×.

Table 1. Adsorbent surface properties by surface area analyzer.

Adsorbents	Surface area (m^2/g)	Pore volume (cc/g)	Average pore diameter (Å)
Eggshells	2.713	1.871×10^{-2}	2.758×10^{2}
Ca-alginate	10.58	4.593×10^{-2}	1.736×10^{2}
EACs	6.102	2.847×10^{-2}	1.866×10^{2}

enhanced surface area of the EACs, as evidenced by the significantly larger surface area (6.102 m^2/g) compared to that of the eggshells.

The BET method utilized in the surface area analysis allows for the determination of the specific surface area of the adsorbent, providing valuable insights into its potential adsorption capacity. Furthermore, the BJH analysis offers information about the pore volume and distribution within the adsorbent material.

Based on the findings from the surface area analysis, it can be concluded that the synthesized EACs possess a desirable mesoporous structure, contributing to their higher surface area when compared to the original eggshell material. This increased surface area indicates a greater potential for adsorption and underscores the effectiveness of EACs as an adsorbent in various applications.

3.2. Sorption studies

3.2.1. Effect of composition and contact time on RhB adsorption onto EACs

To determine the effect of composition and contact time on the adsorption of RhB by EACs, 25 mL of 20 ppm RhB solution was made in contact with 0.1 g of adsorbent at room temperature and a stirring speed of 100 rpm. The adsorbents used were eggshell powder, Ca-Alginate, Eggshells-Alginate (EACs) 1:1, EACs 1:2, EACs 1:4, EACs 2:1, and EACs 4:1. The contact time was varied from 15 min to 240 min.

From Fig. 4, it can be seen that EACs with a ratio of 2:1 has the largest adsorption capacity. However, the continuous addition of eggshell powder until it reaches an eggshell-alginate ratio of 4:1 can result in the size of the EACs being larger than before which results in a lower surface area of the adsorbent. Moreover, it can also be seen from the figure that in all variations of adsorbent composition, the adsorption capacity of EACs for RhB increases rapidly in the first 50 min and continued to increase until it reaches the adsorption equilibrium at 180 min then the curve becomes relatively flat afterward. The results imply that the adsorbent is saturated and is difficult to adsorb RhB molecules after 180 min.

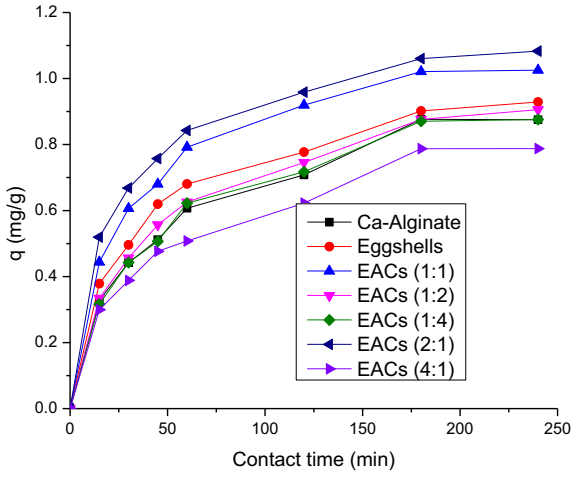

Fig. 4. Effect of contact time on RhB removal (initial dye concentration 20 ppm; agitation speed 100 rpm).

3.2.2. Effect of pH

The effect of pH was evaluated at pH values of 2.0, 3.0, 4.0, 5.0, 6.0, and 7.0. The results showed that the higher the pH, the higher the adsorption capacity of EACs for RhB. This is related to the ionic state of the alginate in the EACs at a certain pH. Guluronic acid and mannuronic acid have pKa values of 3.65 and 3.38, respectively. At a pH above the pKa value, the alginate is deprotonated and negatively charged which increases the adsorption capacity of EACs for RhB. However, after reaching around pH 4, the adsorption capacity tends to decrease with increasing pH which can be attributed to the low electrostatic interactions between RhB molecules and the adsorbent.

3.2.3. Effect of adsorbent dosage

The effect of EACs dosage on the adsorption capacity was investigated by contacting 25 mL of 20 ppm RhB solution to the adsorbent for 180 min at 25 ± 0.5 °C with an agitation speed of 100 rpm and pH 4. Different amounts of adsorbents (0.05, 0.1, 0.25, 0.5, 0.75, 1 g) were added to the solution. From Fig. 5, it is obvious that increasing EACs dosage at constant RhB concentration resulted in a decrease in adsorption capacity which could be attributed to the saturation of the adsorption sites mainly due to particle interactions.

3.2.4. Effect of initial concentration

The effect of initial concentration on RhB adsorption by EACs was investigated by contacting 0.1 g of EACs with 25 mL of RhB solution with varying concentrations in the range of 5–500 ppm at pH 4 with an agitation speed of 100 rpm for 180 min and a temperature of 25 ± 0.5 °C.

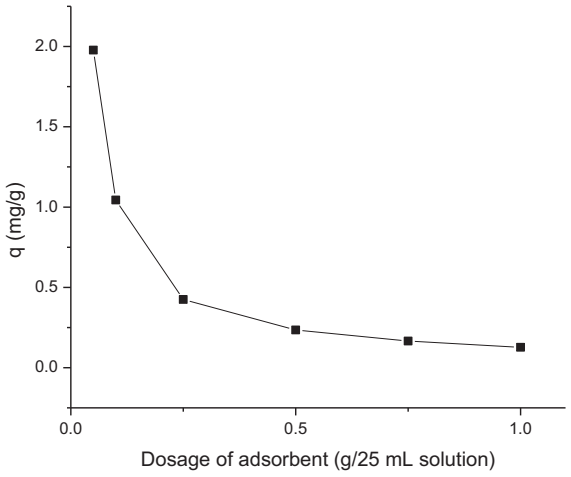

Fig. 5. Effect of adsorbent dosage on adsorption capacity ((initial dye concentration 20 ppm; agitation speed at 100 rpm for 180 min; pH 4).

From Fig. 6 it can be seen that the higher the initial concentration in contact with the adsorbent, the higher the adsorption capacity of EACs for RhB. This is because, at higher concentrations, the number of RhB molecules in the solution becomes larger which makes the opportunity for RhB molecules to interact with the active site on the EACs greater than at low concentrations. However, at a concentration of 400–500 ppm, there was no significant increase in adsorption capacity because the EACs had reached the saturation point.

3.3. Adsorption isotherm studies

In this study, equilibrium data were analyzed using Langmuir, Freundlich, and Sips isotherms models to predict the validity of experimental data. Langmuir's isotherm theory assumes that a surface consisting of identical sites leads to the formation of a monolayer of adsorbate over a homogeneous adsorbent surface. Langmuir adsorption isotherm is described by the following equation [18,19]:

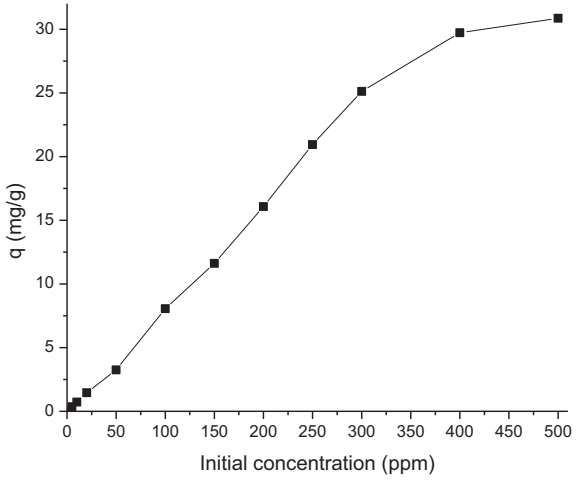

Fig. 6. Effect of initial concentration on adsorption capacity (adsorbent dosage 0.1 g; agitation speed at 100 rpm for 180 min; pH 4).

$$\frac{1}{q_e}=\frac{1}{(K_L q_m)C_e}+\frac{1}{q_m} \tag{2}$$

where q_e is the amount of RhB adsorbed per unit weight of adsorbent (mg g^{-1}), q_m is the maximum adsorption capacity (mg g^{-1}), K_L is the Langmuir constant (L mg^{-1}), and C_e is the adsorbate concentration at equilibrium (mg L^{-1}).

For comparison purposes, the experimental dye adsorption values were also analyzed using the Freundlich equation. The Freundlich adsorption isotherm model assumes a non-uniform distribution on the surface of the adsorbent leading to the formation of a heterogeneous adsorbate layer. This isotherm model can be expressed by the equation below [20].

$$log\, q_e = log\, K_F + \frac{(log\, C_e)}{n} \tag{3}$$

where K_F (mg^{1-n} L^n g^{-1}) and n are Freundlich's adsorption constants related to adsorption capacity and system heterogeneity, respectively.

The Sips model is a combination of the Langmuir and Freundlich isotherm models to predict the behavior of heterogeneous adsorption systems. At low adsorbate concentrations, the Sips isotherm model follows the Freundlich model, while at high adsorbate concentrations, it follows the Langmuir model [21] The Sips equation is represented by equation (4) [22].

$$\log\left(\frac{q_e}{(q_m-q_e)}\right)=\frac{1}{n}log\, C_e + log\, K_S \tag{4}$$

where K_S ($mg^{-1/n}$ $L^{-1/n}$) is Sip's adsorption constants and n is adsorption intensity. To determine the type of isotherm model that is suitable for RhB adsorption by EACs, linearity studies were carried out for the three isotherm models and the results can be seen in Table 2.

Table 2 presents the correlation coefficients (R^2) for the Langmuir, Freundlich, and Sips isotherm models applied to the adsorption of RhB onto EACs. The Langmuir model exhibits a higher correlation coefficient ($R^2 = 0.9995$) compared to the Freundlich model ($R^2 = 0.9925$) and the Sips model ($R^2 = 0.9788$). This suggests that the Langmuir isotherm model provides a better fit to the equilibrium data, indicating that the adsorption of RhB on EACs follows a monolayer adsorption process.

Table 2. Isotherm parameters of three models for RhB adsorption using EACs.

Langmuir		
K_L *(L/mg)*	q_m *(mg/g)*	R^2
0.1	151.51	0.9995
Freundlich		
n	K_F*(mg/g)*	R^2
0.9829	0.099	0.9925
Sips		
K_{eq} *(mL/g)*	n	R^2
0.0012	0.7388	0.9788

Fig. 7 illustrates the comparison of the adsorption isotherm curves for RhB removal using EACs. It is evident from the figure that the experimental data align well with the Langmuir adsorption isotherm model, further supporting the appropriateness of this model for describing the adsorption process. The adsorption capacity of EACs for RhB is determined to be 151.51 mg/g, with a relative standard deviation (RSD) value of 0.552%.

The high correlation coefficient (R^2) for the Langmuir model, the good fit between the experimental data and the Langmuir adsorption isotherm curve, and the low RSD value indicate that the adsorption of RhB onto EACs occurs through a homogenous monolayer adsorption mechanism. This finding underscores the effectiveness of EACs as adsorbents for the removal of RhB from aqueous solutions.

Overall, the results obtained from the comparison of adsorption isotherm models and the analysis of the adsorption isotherm curves confirm the favorable performance of EACs in adsorbing RhB, with the Langmuir isotherm model providing the most accurate description of the adsorption process.

3.4. Effect of temperatures and thermodynamics study

The effect of temperature on the adsorption capacity of EACs for RhB was investigated by contacting a 15 mL RhB solution with a concentration range of 5–500 ppm with 0.1 g of EACs at pH 4 with a stirring speed of 100 rpm for 180 min. The contact process was carried out at 3 different temperatures, 26 °C (299 K), 45 °C (318 K), and 60 °C (333 K). These data were then used to obtain information on the thermodynamics of RhB adsorption by EACs.

Enthalpy change (ΔH^o) and entropy change (ΔS^o) as thermodynamic parameters can be determined using the van't Hoff equation below.

$$\ln K_L = \frac{\Delta S^o}{R} - \frac{\Delta H^o}{RT} \tag{5}$$

where K_L is the Langmuir isotherm constant (L/mg), R is the universal gas constant (8.314 J/mol.K), and T is the temperature (K).

The van't Hoff plot ln K_L versus $1/T$ in Fig. 8 provides a straight line with an acceptable correlation coefficient (R^2) and can be used to determine the ΔH^o and ΔS^o values from the slope and intercept of the plot, respectively. The change in Gibbs free energy (ΔG^o) in the RhB adsorption process by EACs can be calculated from the equation below.

$$\Delta G^o = \Delta H^o - T\Delta S^o \tag{6}$$

where ΔG^o is the change in standard free energy (J/mol), ΔH^o is the enthalpy change (J/mol), T is the temperature (K), and ΔS^o is the entropy change (J/mol.K). The thermodynamic parameter values for

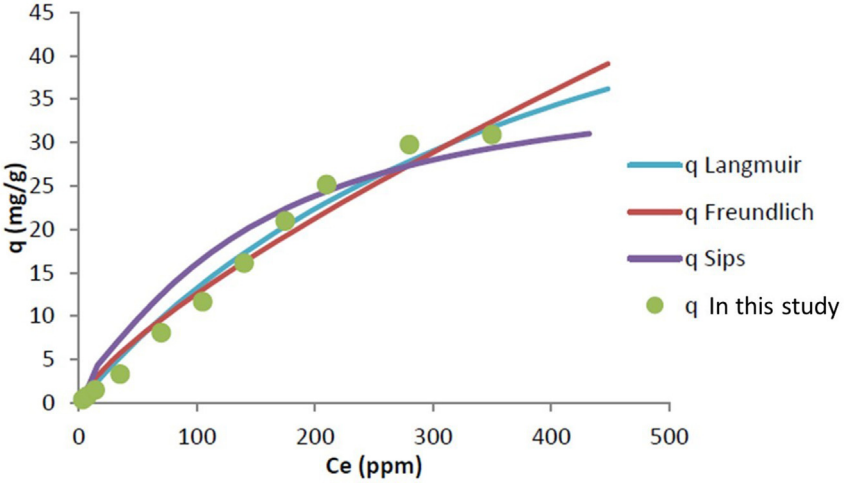

Fig. 7. Non-linear equilibrium plots for RhB removal using EACs (pH = 4, agitation speed = 100 rpm, EACs dosage = 0.1 g, contact time = 180 min).

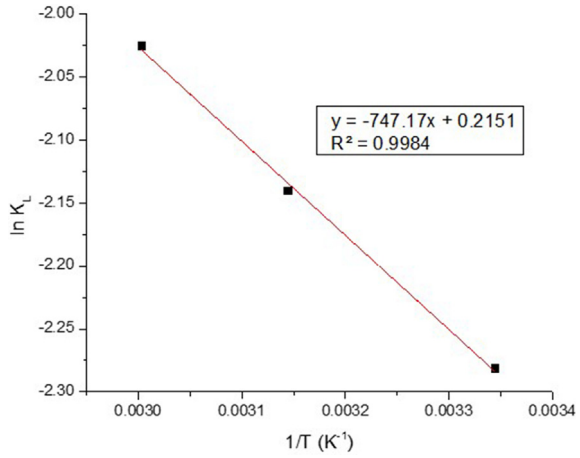

Fig. 8. Van't Hoff plot for RhB removal using EACs at different solution temperatures (pH = 4, agitation speed = 100 rpm, EACs dosage = 0.1 g, contact time = 180 min.

RhB adsorption by EACs at different solution temperatures are listed in Table 3.

The thermodynamic analysis provides valuable insights into the adsorption process of RhB onto EACs. The negative value of ΔH^o (−6.211 kJ/mol) indicates that the adsorption is exothermic, meaning that heat is released during the adsorption process. This suggests that the interaction between RhB and EACs involves a favorable and energetically stable binding.

Moreover, the positive value of ΔS^o (1.788 J/mol·K) indicates an increase in the degree of disorder at the solid–liquid interface during the adsorption process. This suggests that the adsorption of RhB onto EACs involves an increase in randomness or freedom of movement at the molecular level, which is typical for physical adsorption.

The negative values of ΔG^o demonstrate the feasibility and spontaneity of the adsorption process within the studied temperature range. This implies that the adsorption of RhB onto EACs occurs spontaneously without the need for external energy input. Furthermore, it is noteworthy that the change in free energy (ΔG^o) decreases with increasing temperature. This observation suggests that higher temperatures promote a more favorable adsorption process, leading to an increase in the adsorption capacity of EACs for RhB. This behavior can be attributed to enhanced molecular interactions and improved diffusion of RhB molecules onto the adsorbent surface at higher temperatures.

Table 3. Parameters of RhB adsorption thermodynamics by EACs.

T (K)	ΔH^o (kJ/mol)	ΔS^o J/mol.K	ΔG^o (kJ/mol)
299			−6.746
318	−6.211	1.788	−6.780
333			−6.807

3.5. Kinetics studies

In this study, kinetic studies were conducted to investigate the adsorption of RhB onto EACs as a function of concentration and contact time. The concentrations of RhB used ranged from 50 ppm to 500 ppm, and the contact times varied from 15 to 180 min. The kinetic behavior of the adsorption process was analyzed by plotting ln (qe-q) against time for different RhB concentrations, as shown in Fig. 9. It can be observed from the plot that the adsorption of RhB onto EACs does not follow the pseudo-first-order rate kinetics. The pseudo-first-order model equation, represented by a linear equation, can be described as [23].

$$\ln(q_e - q_t) = ln\, q_e - k_1 t \quad (7)$$

where q_t and q_e (mg g^{-1}) are the binding amounts of MIP-NFs and NIP-NFs at contact time (t) and the

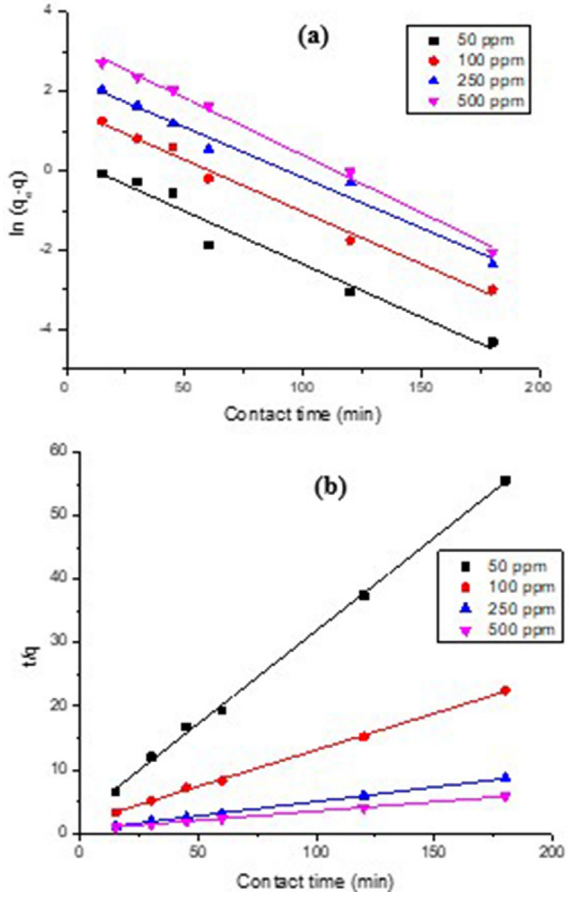

Fig. 9. a) Pseudo-first-order and b) pseudo-second-order plots for different initial dye concentrations removal using EACs (pH = 4, agitation speed = 100 rpm, EACs dosage = 0.1 g).

equilibrium adsorption capacity of MIP-NFs and NIP-NFs, respectively, k_1 (min^{-1}) is the pseudo-first-order kinetic constant.

The pseudo-second-order model assumes that the adsorption rate is directly proportional to the square of the adsorbate's quantity on the surface of the adsorbent [24]. The linear equation representing the pseudo-second-order kinetic model can be expressed as follows.

$$\frac{t}{q_t}=\frac{1}{(k_2 q_e^2)}+\frac{t}{q_e} \quad (8)$$

where t is the contact time (min), qt is the amount of adsorbate adsorbed at time t (mg/g), qe is the equilibrium adsorption capacity (mg/g), and k is the pseudo-second-order rate constant (g/mg·min). This model provides a better fit for the experimental data and allows for a more accurate prediction of the adsorption behavior of RhB onto EACs.

The parameter values and correlation coefficients of each adsorption kinetics are presented in Table 4. The obtained correlation coefficients for the pseudo-second-order kinetic model are all greater than 0.99, indicating a strong fit between the experimental data and the model. This suggests that the adsorption kinetics of RhB by EACs can be accurately described by the pseudo-second-order model. The high correlation coefficients validate the hypothesis that the adsorption of RhB onto EACs involves a chemical adsorption process. It indicates that the RhB molecules in the solution form chemical bonds with the adsorbent, leading to a strong attachment between the dye molecules and the EACs surface.

3.6. Comparison to other adsorbents

The maximum adsorption capacities of RhB reported for various low-cost and environmentally friendly adsorbents are summarized in Table 5. It can be observed that the adsorption capacities vary for each type of adsorbent due to their distinct characteristics. In comparison to other adsorbents, EACs exhibit a relatively high maximum adsorption capacity value. This suggests that EACs possess a strong potential for further development as effective adsorbents for the removal of RhB from wastewater.

Table 4. Pseudo-first-order and pseudo-second-order parameter values.

RhB concentration (ppm)	Pseudo-first-order		Pseudo-second-order	
	R^2	k_1 (min^{-2})	R^2	k_2 (min.g/mg)
50	0.9960	2.88×10^{-2}	0.9985	3.574×10^{-2}
100	0.9794	2.54×10^{-2}	0.9989	9.299×10^{-3}
250	0.9898	2.62×10^{-2}	0.9997	4.759×10^{-3}
500	0.9623	2.67×10^{-2}	0.9994	1.859×10^{-3}

Table 5. Low-cost materials as adsorbents for RhB.

Adsorbent	q_m (mg/g)	References
Pomegranate peel	30.47	[22]
Commercial Activated Carbon	46.2	[25]
Black tea leaves	53.2	[26]
Biochar obtained from hydrochar pyrolysis using bamboo shoot shells	85.8	[27]
Modified banyan aerial roots	115.23	[28]
Hydrothermally synthesized zinc oxide-loaded activated carbon (ZnO-AC)	128.2	[29]
Waste of seeds of Aleurites Moluccana,	178	[30]
Eggshells-alginate composites	151.51	**this study**

The favorable adsorption capacity of EACs suggests their suitability for addressing the challenge of RhB contamination in water treatment processes.

4. Conclusion

In conclusion, this study successfully synthesized and characterized eggshell-alginate composites (EACs) and evaluated their efficacy as adsorbents for Rhodamine B (RhB) removal. TGA analysis confirmed the superior thermal resistance of EACs compared to Ca-alginate. The BET method revealed a substantial surface area of 6.102 m^2/g for EACs, while the BJH method highlighted their abundance of mesopores. The adsorption capacity of EACs for RhB was found to be influenced by various factors, including contact time, pH, adsorbent dose, and RhB concentration. Notably, EACs exhibited a maximum adsorption capacity of 151.51 mg/g, following the pseudo-second-order kinetics model and Langmuir adsorption isotherm. The negative value of ΔH^o indicated an exothermic adsorption process, while the positive value of ΔS^o suggested an increasing degree of disorder at the solid–liquid interface. Furthermore, the negative values of ΔG^o confirmed the feasibility and spontaneous nature of the adsorption process within the studied temperature range. Compared to other adsorbents, EACs demonstrated a relatively high maximum adsorption capacity, underscoring their promising potential for RhB removal from wastewater.

Conflicts of interest

The authors declare no competing interests.

Acknowledgement

The authors are very grateful to the Faculty of Mathematics and Natural Science, Bandung Institute of Technology, for the financial support for this

research through the Research, Community Service, and Innovation (PPMI) funding.

References

[1] A. Kausar, R. Shahzad, S. Asim, S. BiBi, J. Iqbal, N. Muhammad, I.U. Din, Experimental and theoretical studies of Rhodamine B direct dye sorption onto clay-cellulose composite, J. Mol. Liq. 328 (2021) 115165, https://doi.org/10.1016/j.molliq.2020.115165.

[2] A. Kausar, Research progress in frontiers of poly(ionic Liquid)s: a review, Polym. Plast. Technol. Eng. 56 (2017) 1823–1838, https://doi.org/10.1080/03602559.2017.1289410.

[3] P. Deng, J. Xiao, J. Chen, J. Feng, Y. Wei, J. Zuo, J. Liu, J. Li, Q. He, Polyethylenimine-carbon nanotubes composite as an electrochemical sensing platform for sensitive and selective detection of toxic rhodamine B in soft drinks and chilli-containing products, J. Food Compos. Anal. 107 (2022) 104386, https://doi.org/10.1016/j.jfca.2022.104386.

[4] Y. Song, K. Wang, F. Zhao, Z. Du, B. Zhong, G. An, Preparation of powdered activated carbon composite material and its adsorption performance and mechanisms for removing RhB, Water 14 (2022) 3048, https://doi.org/10.3390/w14193048.

[5] M. Saleh, M. Yalvaç, H. Arslan, Optimization of remazol brilliant blue R adsorption onto Xanthium italicum using the response surface method, Karbala J. Mod. Sci. 5 (2019) 54–63, https://doi.org/10.33640/2405-609X.1017.

[6] J. Zhang, H. Tong, W. Pei, W. Liu, F. Shi, Y. Li, Y. Huo, Integrated photocatalysis-adsorption- membrane separation in rotating reactor for synergistic removal of RhB, Chemosphere 270 (2021) 129424, https://doi.org/10.1016/j.chemosphere.2020.129424.

[7] H. Li, Z. Wang, Y. Lu, S. Liu, X. Chen, G. Wei, G. Ye, J. Chen, Microplasma electrochemistry (MIPEC) methods for improving the photocatalytic performance of g-C3N4 in degradation of RhB, Appl. Surf. Sci. 531 (2020) 147307, https://doi.org/10.1016/j.apsusc.2020.147307.

[8] S. Chen, M. Liying, D. Yaguang, W. Zhan, T.C. Zhang, D. Du, Highly efficient degradation of rhodamine B by carbon nanotubes-activated persulfate, Sep. Purif. Technol. 256 (2021) 117788, https://doi.org/10.1016/j.seppur.2020.117788.

[9] M. Tuzen A. Sarõ, T.A. Saleh, Response surface optimization, kinetic and thermodynamic studies for effective removal of rhodamine B by magnetic AC/CeO2 nanocomposite, J. Environ. Manage. 206 (2018) 170–177, https://doi.org/10.1016/j.jenvman.2017.10.016.

[10] A.M. Alswieleh, Kinetic, equilibrium and thermodynamic studies for rhodamine B adsorption on sodium taurooglycocholate functionalized mesoporous silica nanoparticles, J. Porous Mater. 30 (2023) 937–948, https://doi.org/10.1007/s10934-022-01395-y.

[11] T.T.N. Phan, A.N. Nikoloski, P.A. Bahri, D. Li, Enhanced removal of organic using LaFeO3-integrated modified natural zeolites via heterogeneous visible light photo-Fenton degradation, J. Environ. Manage. 233 (2019) 471–480, https://doi.org/10.1016/j.jenvman.2018.12.051.

[12] V. Katheresan, J. Kansedo, S.Y. Lau, Efficiency of various recent wastewater dye removal methods: a review, J. Environ. Chem. Eng. 6 (2018) 4676–4697, https://doi.org/10.1016/j.jece.2018.06.060.

[13] N.A. Bakar, A.I.N. Afendi, N.N. Mustaza, N.A.A. Bahman, Methylene blue adsorption by using eggshells in synthetic solution, Multidiscip. Appl. Res. Innov. 2 (2021) 175–182, https://doi.org/10.30880/mari.2021.02.02.022.

[14] J.I. Lee, J.M. Kim, S.C. Yoo, E.H. Jho, C.G. Lee, S.J. Park, Restoring phosphorus from water to soil: using calcined eggshells for P adsorption and subsequent application of the adsorbent as a P fertilizer, Chemosphere 287 (2022) 132267, https://doi.org/10.1016/j.chemosphere.2021.132267.

[15] M. Kalbarczyk, A. Szcześ, Potential biomedical application of calcium phosphates obtained using eggshells as a biosource of calcium at different initial pH values, Ceram. Int. 47 (2021) 33687–33696, https://doi.org/10.1016/j.ceramint.2021.08.278.

[16] M. Madsen, P. Westh, S. Khan, R. Ipsen, K. Almdal, F.L. Aachmann, B. Svensson, Impact of alginate mannuronic-guluronic acid contents and pH on protein binding capacity and complex size, Biomacromolecules 22 (2021) 649–660, https://doi.org/10.1021/acs.biomac.0c01485.

[17] F. Xu, Q.Q. Cha, Y.Z. Zhang, X.L. Chen, Degradation and utilization of alginate by marine Pseudoalteromonas: a Review, Appl. Environ. Microbiol. 87 (2021) 1–17, https://doi.org/10.1128/AEM.00368-21.

[18] A. Esra, M. Yenigun, A. Sarõ, H. Altundag, M. Tuzen, T.A. Saleh, Facile synthesis of zinc oxide nanoparticles loaded activated carbon as an eco-friendly adsor bent for ultra-removal of malachite green from water, Environ. Technol. Innov. 21 (2021) 101305, https://doi.org/10.1016/j.eti.2020.101305.

[19] J. Shi, H. Zhang, Y. Yu, X. Zou, W. Zhou, J. Guo, Y. Ye, Y. Zhao, Adsorption properties of calcium alginate-silica dioxide hybrid adsorbent to methylene blue, J. Inorg. Organomet. Polym. Mater. 30 (2020) 2114–2125, https://doi.org/10.1007/s10904-019-01357-z.

[20] N. Yuan, H. Cai, T. Liu, Q. Huang, X. Zhang, Adsorptive removal of methylene blue from aqueous solution using coal fly ash-derived mesoporous silica material, Adsorpt. Sci. Technol. 37 (2019) 333–348, https://doi.org/10.1177/0263617419827438.

[21] M.A. Zulfikar, H. Setiyanto, Rusnadi, L. Solakhudin, Rubber seeds (Hevea brasiliensis): an adsorbent for adsorption of Congo red from aqueous solution, Desalin. Water Treat. 56 (2015) 2976–2987, https://doi.org/10.1080/19443994.2014.966276.

[22] R. Chakraborty, A. Asthana, A.K. Singh, S. Yadav, Md A.H. Susan, S.A.C. Carabineiro, Intensified elimination of aqueous heavy metal ions using chicken feathers chemically modified by a batch method, j. Mol. Liq. 312 (2020) 113475, https://doi.org/10.1016/j.molliq.2020.113475.

[23] R. Chakraborty, R. Verma, A. Asthana, S.S. Vidya, A.K. Singh, Adsorption of hazardous chromium (VI) ions from aqueous solutions using modified sawdust: kinetics, isotherm, and thermodynamic modelling, Int. J. Environ. Anal. Chem. 101 (2021) 911–928, https://doi.org/10.1080/03067319.2019.1673743.

[24] R. Ghibate, O. Senhaji, R. Taouil, Kinetic and thermodynamic approaches on Rhodamine B adsorption onto pomegranate peel, Case Stud. Chem. Environ. Eng. 3 (2021) 100078, https://doi.org/10.1016/j.cscee.2020.100078.

[25] Y. Li, X. Yan, X. Hu, R. Feng, M. Zhou, Trace pyrolyzed ZIF-67 loaded activated carbon pellets for enhanced adsorption and catalytic degradation of Rhodamine B in water, Chem. Eng. J. 375 (2019) 122003, https://doi.org/10.1016/j.cej.2019.122003.

[26] M.A. Hossain, M.S. Alam, Adsorption kinetics of Rhodamine-B on used black tea leaves, Iranian J. Environ. Health Sci. Eng. 9 (2012) 1–7, https://doi.org/10.1186/1735-2746-9-2.

[27] Y. Hou, G. Huang, J. Li, Q. Yang, S. Huang, J. Cai, Hydrothermal conversion of bamboo shoot shell to biochar: preliminary studies of adsorption equilibrium and kinetics for rhodamine B removal, J. Anal. Appl. Pyrolysis. 143 (2019) 104694, https://doi.org/10.1016/j.jaap.2019.104694.

[28] H. Fan, Y. Ma, J. Wan, Y. Wang, Removal of gentian violet and rhodamine B using banyan aerial roots after modification and mechanism studies of differential adsorption behaviors, Environ. Sci. Pollut. Res. 27 (2020) 9152–9166, https://doi.org/10.1007/s11356-019-07024-7.

[29] J. Saini, V.K. Garg, R.K. Gupta, N. Kataria, Removal of Orange G and Rhodamine B dyes from aqueous system using hydrothermally synthesized zinc oxide loaded activated carbon (ZnO-AC), J. Environ. Chem. Eng. 5 (2017) 884–892, https://doi.org/10.1016/j.jece.2017.01.012.

[30] D.L. Postai, C.A. Demarchi, F. Zanatta, D.C.C. Melo, C.A. Rodrigues, Adsorption of rhodamine B and methylene blue dyes using waste of seeds of Aleurites Moluccana, a low-cost adsorbent, Alexandria Eng. J. 55 (2016) 1713–1723, https://doi.org/10.1016/j.aej.2016.03.017.